Journal of Structural Geology, Vol. 10, No. 5, pp. 499 to 515, 1988
Printed in Great Britain

0191-8141/88 $03.00 + 0.00

Tectonic processes in a surge-type glacier

MARTIN SHARP, WENDY LAWSON

Department of Geography, University of Cambridge, Downing Place, Cambridge CB2 3EN, U.K.

and

ROBERT S. ANDERSON

Division of Physics, Mathematics and Astronomy 200–36, California Institute of Technology
Pasadena, CA 91125, U.S.A.

(*Received* 2 *July* 1987; *accepted in revised form* 7 *March* 1988)

Abstract—The 1982–1983 surge of Variegated Glacier involved the development, growth and downglacier propagation of a velocity peak associated with rapid basal sliding facilitated by high subglacial water pressures. Passage of the velocity peak through the glacier was preceded by an episode of longitudinal shortening and followed by an episode of elongation. The deformation history of the glacier ice was dependent upon location relative to the surge nucleus and the final position reached by the propagating velocity peak. Ice above the surge nucleus experienced continuous and cumulative elongation; ice below the final position of the velocity peak experienced continuous and cumulative shortening; ice between these two points experienced shortening followed by elongation and low cumulative strain. The large-scale pattern of ice structure development reflects these deformation histories. Surging is equivalent to thrust sheet emplacement by a combination of gravity gliding over a weakened basal layer and 'push from behind', with the gravity-driven motion of the surging part of the glacier providing the push which allows the surge front to propagate. The relationships established between the deformation history of surging glaciers and the development of ice structures may facilitate the interpretation of structures in thrust sheets.

INTRODUCTION

THRUST sheets and nappes are usually considered to have been emplaced by one of the following mechanisms (Price & McClay 1981):

(1) the structures were 'pushed from behind';

(2) the structures were emplaced by gliding down an inclined plane under the action of gravity;

(3) the structures were emplaced by gravitational spreading, possibly accompanied by an initial phase of diapirism.

In most settings of geological interest, however, the rates of emplacement are too slow to allow direct observation, and mechanisms of emplacement must be inferred from the structures and strain histories of deformed rocks. By contrast, ice in non-surging glaciers undergoes the cycle of deposition, burial, diagenesis, metamorphism, fracture and flow about 6 orders of magnitude faster than the Mesozoic sediments of the Alpine orogenic belt (Hambrey & Milnes 1977). Glaciers can therefore serve as excellent laboratories for the study of the mechanisms of rock deformation. In most cases, however, the flow of glaciers is approximately steady over long periods of time, being sustained by the addition of material by accumulation in the upper reaches and its removal by ablation in the lower reaches. Normal glacier flow, therefore, differs in important ways from the emplacement of nappes which involve finite amounts of rock material and discrete deformation events. A small proportion of contemporary glaciers, however, exhibit a type of behaviour known as 'surging' (Meier & Post 1969) which may be more closely analogous to the processes by which thrust sheets are emplaced. Study of the structures developed in surge-type glaciers and their relationship to the deformation history of the ice may therefore facilitate the inference of mechanisms of thrust sheet emplacement from geological structures.

Glacier surges are periodically recurring episodes of rapid ice motion, some of which lead to glacier advances. Velocities during surges may reach 100 times normal flow velocities and they are achieved by rapid basal sliding made possible by high subglacial water pressures (Kamb *et al.* 1985). Surges initiate in a localized nucleus zone, from which they may propagate both up- and downglacier (McMeeking & Johnson 1986, Raymond 1987). Propagation is made possible by the transfer of stress from the rapidly sliding part of the glacier to the more slowly-moving regions around it. This sets up local stress concentrations which enhance ice deformation and generate topographic changes which have a feedback effect on the velocity distribution. The precise mechanisms involved in propagation of a surge are discussed by McMeeking & Johnson (1986) and Raymond *et al.* (1987). Surges transfer large volumes of ice from an upper reservoir area to a lower receiving area, and produce major changes in the appearance of a glacier. They also produce distinctive suites of tectonic structures. In this paper we describe the tectonic processes which occurred during the 1982–1983 surge of

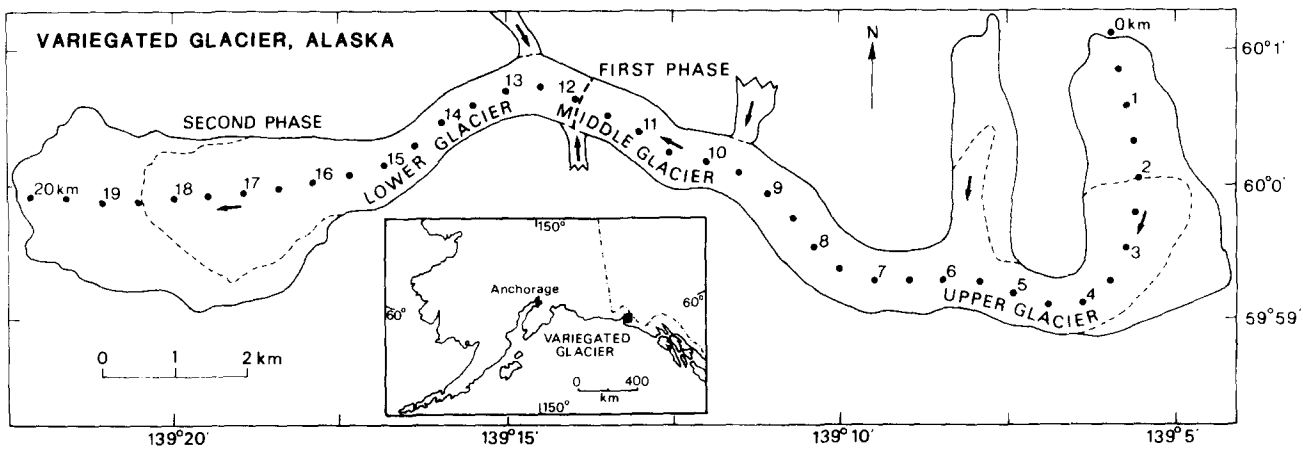

Fig. 1. Map of Variegated Glacier, Alaska, showing the limits of the first and second phases of the 1982–1983 surge and the centreline distance scale by which locations are referenced in the text. Inset shows the location of the glacier.

Variegated Glacier, Alaska (Kamb *et al.* 1985), and discuss the application of these observations to the interpretation of structures in thrust sheets.

VARIEGATED GLACIER

Variegated Glacier is a 20 km long valley glacier located above Russell Fjord on the south side of the St Elias Range in southeastern Alaska (Fig. 1). It has a well-documented history of surging (Bindschadler *et al.* 1977) with five surges occurring at 18–20 yr intervals between 1906 and 1983. Detailed studies carried out since 1973 documented the behaviour of the glacier prior to and during its 1982–1983 surge (Kamb *et al.* 1985, Raymond & Harrison in press). This surge was a two-phase event. The first phase of activity lasted from January to June 1982 and affected a region extending from 2 to 12 km from the head of the glacier (Fig. 1). During the second phase, which lasted from October 1982 until July 1983, the surge propagated into the lower glacier, eventually terminating at a point around 18 km from its head (Kamb *et al.* 1985) (Fig. 1). The surge was therefore initiated in the upper reaches of the glacier, from where it propagated downvalley, developing a dramatic surge front associated with a steep topographic ramp, a sharp jump in horizontal velocity (0–20 m day^{-1} in *ca* 500 m), intense longitudinal compression (peak strain rates in excess of -0.2 day^{-1}) and rapid thickening (peak rates of over 7 m day^{-1}) (Raymond *et al.* 1987). Over the period 20 June–5 July 1983, this front propagated at a rate, $\dot{W}$, of $\simeq$40 m day^{-1}. Assuming that motion in the surge zone is by basal sliding and that deformation is confined to a vertical plane aligned parallel to the ice flow direction, $\dot{W}$ is defined by the requirements of volume conservation:

$$\dot{W} = U_2 h_2/(h_2 - h_1), \qquad (1)$$

where U_2 is the ice velocity above the surge front, and h_2 and h_1 are the ice thicknesses above and below the surge front (Raymond *et al.* 1987). The front therefore moved faster than the ice. Transfer of ice from the reservoir area to the receiving area produced 50 m of thinning at 8 km and 100 m of thickening at 16 km from the head of the glacier. Within the surging part of the glacier 95% of the ice motion was by basal sliding, and subglacial water pressures were always within 400–500 kPa of overburden pressure, occasionally exceeding it (Kamb *et al.* 1985). Within the surge front the basal sliding velocity fell to zero and ice deformation made a more important contribution to the overall velocity (Raymond *et al.* 1987).

KINEMATICS OF THE 1982–1983 SURGE

Ice velocities and displacements

The development of the velocity field during the 1982–1983 surge is shown in Fig. 2, which is derived from data contained in Raymond (unpublished NSF report 1984). During Phase 1 of the surge, there was a general downglacier decrease in surface velocity from a peak 4–5 km from the head of the glacier. Ice below 12 km was unaffected by this phase of motion (Fig. 1). In the early part of the second phase, the velocity peak shifted gradually downglacier, reaching 8 km from the head by March 1983. After this, it began to move much more rapidly and to amplify downglacier. By June 1983 it had reached 15 km and was associated with velocities of the order of 45 m day^{-1}. Velocities dropped off sharply to zero in front of this peak. The surge thus involved the development, growth and downglacier propagation of a distinct velocity peak which became progressively closer to the surge front as it moved downvalley. The surge terminated abruptly over the full length of the glacier on 4–5 July 1983. Results presented in Figs. 2–5 therefore finish on this date.

From the information contained in Fig. 2, we have calculated the trajectories of ice particles starting from points spaced at 2 km intervals down the centreline of the glacier over the region between 4 and 16 km from the head (Fig. 3). Most ice particles starting in the region 4–14 km from the head moved around 2.3 km, with a maximum displacement of around 2.5 km for an ice

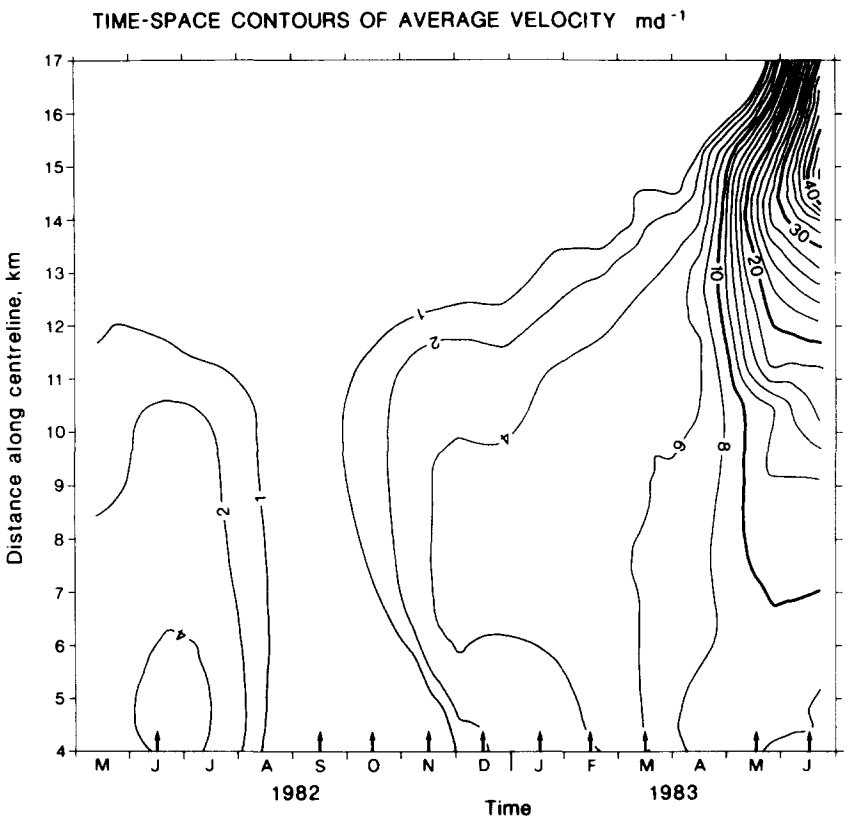

Fig. 2. Space–time evolution of the centreline velocity field during the 1982–1983 surge of Variegated Glacier. Arrows on the horizontal axis delimit the time periods for which calculations were carried out.

particle starting 12 km from the head of the glacier. Ice particles from progressively lower starting points moved later, faster and for shorter periods than those starting near the head of the glacier. Ice particles starting from below 14 km moved shorter distances, however, because of the limited duration of surge activity in this part of the glacier.

Longitudinal strain rates and cumulative strains

Longitudinal strain rates for successive measurement periods were calculated from the changes in spacing of ice particles initially located 2 km apart:

$$\dot{\varepsilon} = (l_1 - l_0)/l_0 \Delta t. \quad (2)$$

Here $\dot{\varepsilon}$ is the strain rate, l_0 and l_1 are the initial and new spacings of adjacent points, and Δt is the time interval between measurements (typically of the order of 1–2 months). Positive values indicate extension, and negative values compression. No account is taken of the effects of burial and exposure of the surface ice by accumulation and ablation, factors which might significantly influence the strain history in the presence of a large vertical velocity gradient. They are not considered to be important here, however, because total accumulation and ablation over the 18 month surge period would be small, and because most of the surge motion occurs by basal sliding, with the result that the vertical velocity gradient in the surging part of the glacier is minimal. The spatial and temporal averaging involved in these calculations undoubtedly underestimates the peak strain rates experienced by the ice but it nevertheless gives a good impression of the general pattern of deformation experienced by ice in different parts of the glacier. It therefore provides a useful basis for the interpretation of the structures which developed during the surge. The strain rates calculated are those aligned on an axis parallel to the direction of ice flow at the centreline of the glacier. Determinations of the orientation of the principal strain rate axes in the centre of the lower glacier in June 1983 suggest that these were aligned approximately parallel to and normal to the ice flow direction (Raymond *et al.* 1987). The strain rates calculated here may therefore approximate one of the principal near-surface strain rates.

Four distinct types of behaviour can be identified from the temporal patterns of strain rates for successive 2 km segments of the glacier (Fig. 4).

(a) Ice starting 4–6 km from the head of the glacier experienced compressive strain rates in the first phase of the surge and then extensional strain rates.

(b) Ice starting 6–12 km from the head experienced two distinct compressive strain events associated with the two surge phases, followed by extension in the latter part of the second phase. For ice starting between 8 and 10 km, the two compressive events were separated by a brief period of extension.

(c) Ice starting 12–14 km from the head experienced a single compressive strain event in the second phase of

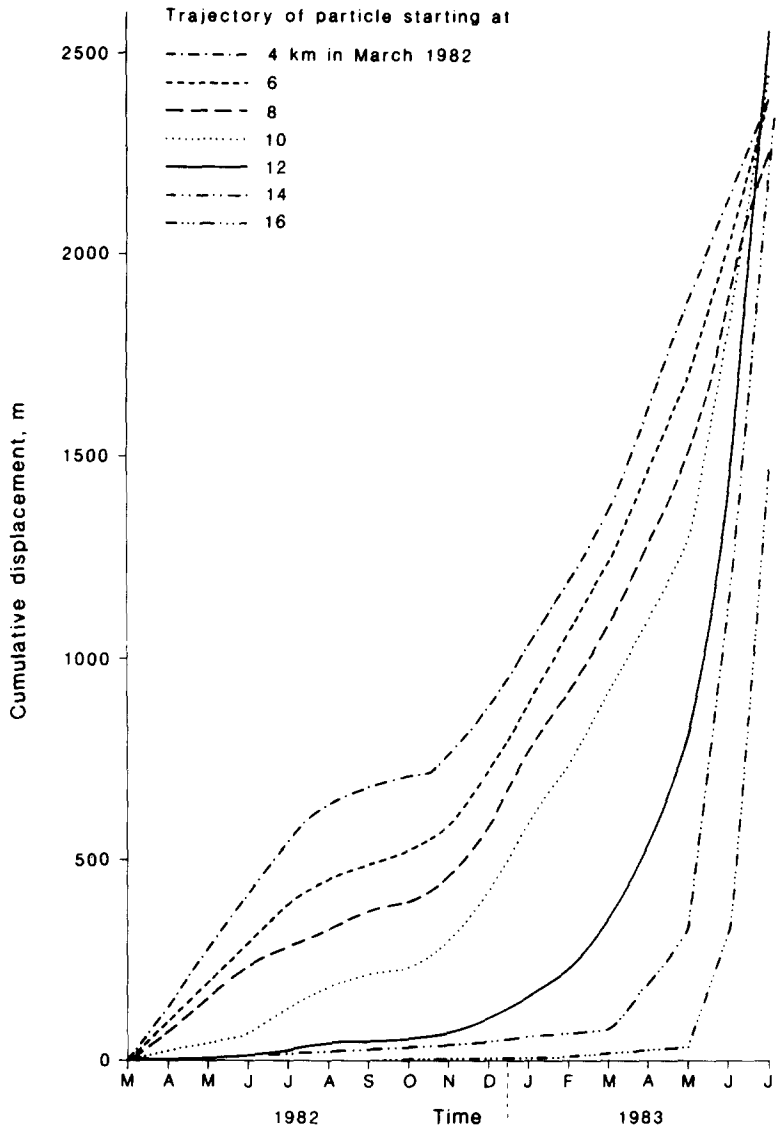

Fig. 3. Trajectories of ice particles starting at 2 km intervals down the centreline of Variegated Glacier during its 1982–1983 surge.

the surge, followed by extension after the passage of the surge front and its associated velocity peak. The ice experienced the greatest rates of longitudinal extension (0.008 day^{-1}) recorded anywhere in the glacier.

(d) Ice starting below 14 km experienced a single large compressive strain event in phase two of the surge. Peak strain rates reached -0.01 day^{-1} (though measurements made over a few hours on smaller parcels of ice recorded rates in excess of -0.2 day^{-1}; Raymond *et al.* 1987).

No data are available for the part of the glacier above 4 km from the head, but aerial photographs show that the dominant structures in this area are transverse crevasses. Since such crevasses tend to open up normal to the orientation of the axis of least compressive strain ($\dot{\varepsilon}_1$) in near-surface ice it is likely that this area always lay above the surge nucleus and that it was always subject to longitudinal extension.

The pattern of deformation experienced by individual ice parcels can thus be understood in terms of their location relative to the original surge nucleus and to the final position reached by the downglacier-propagating velocity peak. Ice located above the surge nucleus was always subject to longitudinal extension; ice located below the nucleus but above the final position reached by the velocity peak was compressed and then extended as the peak passed by; ice located below the final position reached by the surge velocity peak was only compressed. Deformation therefore took the form of a propagating strain wave, with shortening preceding the passage of the surge velocity peak and elongation following it. The magnitude of the deformation rates increased as the amplitude of the velocity peak increased downglacier.

Cumulative strains (ε) from the beginning of the surge were also calculated:

$$\varepsilon = (l_1 - l_0)/l_0, \tag{3}$$

where l_0 is always 2 km. The development of cumulative strain over time shows three distinctive patterns (Fig. 5).

(a) Ice starting between 4 and 10 km from the head experienced early shortening (5–10%), followed by a period during which there was little accumulation of

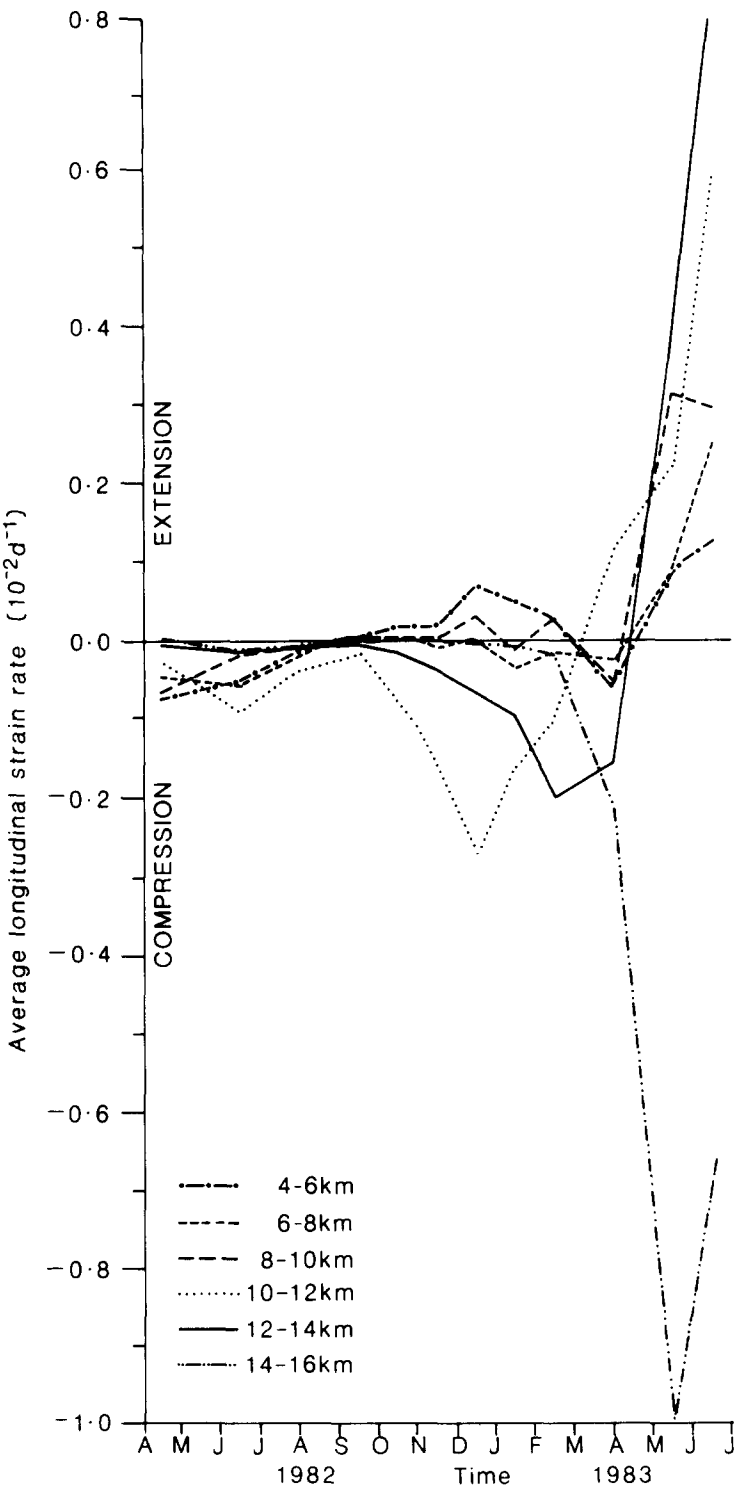

Fig. 4. Longitudinal strain rates for 2 km long parcels of ice located on the centreline of Variegated Glacier during its 1982–1983 surge. Arrows define the time periods on which calculations are based.

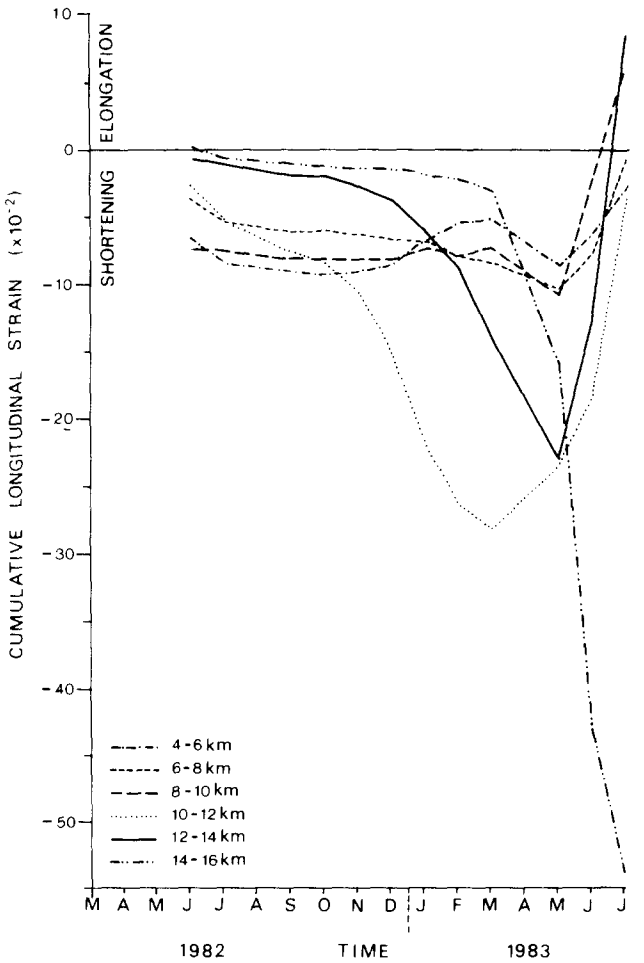

Fig. 5. Longitudinal cumulative strains for 2 km long parcels of ice located on the centreline of Variegated Glacier during its 1982–1983 surge.

strain and finally by a period during which the magnitude of shortening was reduced by elongation. This latter phase actually produced 5% cumulative elongation of ice starting between 8 and 10 km.

(b) Ice starting between 10 and 14 km experienced large shortening (20–30% at peak), but this was later reduced by elongation. Ten per cent cumulative elongation was eventually recorded for ice starting between 12 and 14 km.

(c) Ice starting below 14 km experienced very large cumulative shortening (up to 50% for ice starting between 14 and 16 km).

Thus over most of the glacier cumulative shortening was recorded during the surge. In areas above the final position reached by the velocity peak, however, the final cumulative strain was less than the peak value because some of the initial shortening was undone by the subsequent elongation. Small values of cumulative elongation were recorded for ice parcels starting between 8 and 10, and 12 and 14 km. Cumulative elongation was probably also experienced by ice starting above 4 km from the head, but no data are available. It can thus be seen that in most areas the cumulative strain recorded at the end of the surge is not a good indicator of the strain history. Clearly ice can record cumulative shortening even after it has subsequently experienced prolonged periods of elongation.

STRUCTURES FORMED DURING THE 1982–1983 SURGE

The nature of the structures produced by the surge was determined by direct observation in June and July 1983, and by the analysis of aerial photographs taken at the end of each of the surge phases (Fig. 6).

Transverse fractures

Transverse fractures were the dominant structure developed in the region of extending flow from 2 to 4.5 km below the head of the glacier. Here they were orientated normal to the ice flow direction in the central parts of the glacier, but curved downglacier towards the valley walls. From 4.5 to 15.5 km they were present in association with other fracture sets, but below 15.5 km they were absent. Particularly large transverse chasm sets were developed between 10.5 and 11, and 14 and 15 km in ice which experienced cumulative elongation during the surge (starting at 8.5 and 12 km below the head).

Marginal shear zones

Transverse velocity profiles measured during the surge demonstrate that flow was plug-like, with nearly constant velocities across most of the width of the glacier and intense shear at the margins (Kamb *et al.* 1985). This pattern of velocity is reflected in the formation of marginal shear zones up to 250 m wide on either side of the glacier. In many parts of the glacier the intensity of crevassing within the shear zones was too great to permit reconstruction of fracture patterns from aerial photographs. Study of photographs taken in August 1982 has, however, allowed us to tentatively reconstruct a sequence of structure development in shear zones by looking at the structures found in the poorly developed shear zone on the southern side of the surge front at that time. This sequence seems to begin with the formation of crevasses aligned downglacier at 35° to the ice margin (angles measured anticlockwise from the southern valley wall of the glacier). These crevasses are analogous to tension gashes in shear zones in rocks, and they are rotated by progressive deformation into a form which is convex downglacier. They occur in ice within 100 m of the valley walls, and are succeeded towards the centre of the glacier by a 50 m wide zone of conjugate fractures. The two fracture sets are both aligned downglacier, and initially make angles of 10° and 70° with the valley walls. They thus appear to be Riedel shears. Further towards the centreline again is a zone of fractures aligned at 145° to the valley walls which curve downglacier to join a set of longitudinally-aligned fractures in the central region of the glacier. These sets of structures appear to develop when the ice is accelerated by the arrival of the surge

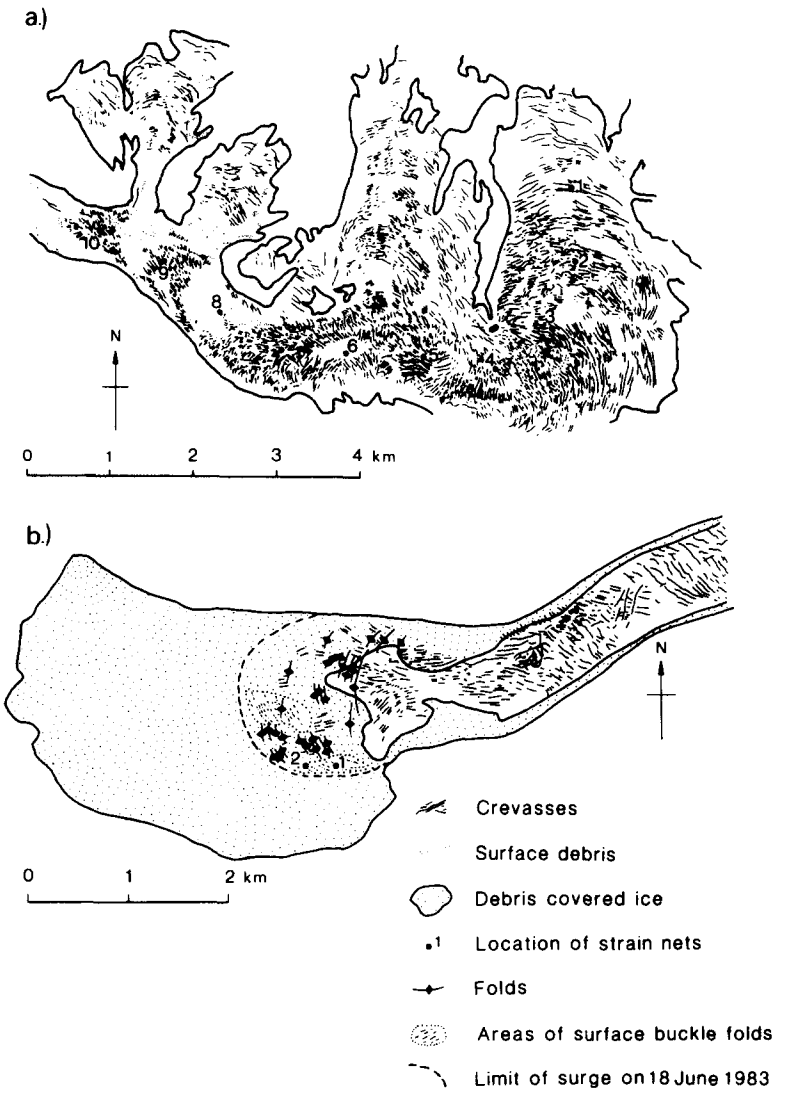

Fig. 6. (a) Pattern of fractures in the upper 12 km of Variegated Glacier at the end of the first phase of its surge (January–June 1982). Centreline distance scale is shown to facilitate comparison with Fig. 1. (b) Structures in the lower reaches of Variegated Glacier at the end of the second phase of its surge (October 1982–July 1983). The map is based on aerial photographs taken on 20 June 1983, only 2 weeks before the end of the surge and it shows the location of strain nets 1 and 2.

front, as the transverse velocity profile is transformed from its parabolic pre-surge form to its plug-like surge form. The marginal crevasses are, however, subsequently overprinted by the formation of a linear zone of brecciated ice approximately 40 m wide located about 50 m from the valley walls. This zone represents the formation of marginal wrench faults associated with the development of a truly plug-like transverse velocity profile as the ice becomes fully incorporated into the surge. In the upper parts of the glacier, lowering of the ice surface took place along these wrench faults, leaving ice blocks stranded on the valley walls up to 50 m above the glacier. Below 16 km, the glacier expanded into a terminal lobe where flow was directed towards rather than parallel to the ice margin. In this area, where valley walls were absent, the marginal wrench faults were replaced by the development of shear folds aligned obliquely to the flow direction (cf. Fischer & Coward 1982).

Longitudinal fractures

Below 15.5 km, where longitudinal shortening produced a surface cross-profile which was strongly convex upwards, the dominant fracture set was aligned parallel to the ice flow direction (Fig. 6b). This fracture set was also present in the reach 4.5–15.5 km, where it intersected the transverse fracture set, but it was absent above 4.5 km. Longitudinal fractures were expanded into enormous chasms in the region 15.5–17 km, the part of the glacier which experienced maximum cumulative shortening during the surge. Below 17 km these fractures tended to occur in transversely-aligned groups. These groups were associated with large concentric folds on the ice surface, the vertical fractures developing on the downglacier limb of the folds, aligned normal to the fold axes. In many cases, ice blocks between fractures were buckled by subsequent shortening parallel to the flow direction, while some fractures showed evidence of

strike-slip displacement leading to the formation of sheared snow-bridges.

Surface folds

Two types of folds developed on the surface of the lower glacier as it was activated by the surge front in the summer of 1983. We term these 'bulge folds' and 'exfoliation buckle folds'. They formed by two distinct mechanisms: ductile flow (Hudleston 1977) and creep buckling (Collins & McCrae 1985). Bulge folds were cylindrical folds up to 20 m high, the axes of which were orientated approximately normal to the ice flow direction. They appeared to develop by the amplification of pre-existing topographic irregularities such as ice-cored moraines as these features were compressed by the arrival of the surge front. If transverse strain is negligible, amplification of pre-existing irregularities is to be expected because the rate of ice thickening, $\dot{V}$, is given by:

$$\dot{V} = \dot{\varepsilon}h, \tag{4}$$

where h is the ice thickness and $\dot{\varepsilon}$ the longitudinal strain rate. For a given strain rate, therefore, there will be preferential thickening of areas of locally thicker ice such as might occur beneath local topographic highs. Some bulge folds also seemed to develop as hangingwall anticlines above the tips of thrust faults (Fig. 7a). Such folds were frequently overturned, verging downglacier, with fracture sets developed on their downglacier limbs which permitted the spalling of large ice blocks and the build-up of an ice-block breccia. This was subsequently bulldozed in front of the advancing nappe as it broke out above the thrust fault.

Exfoliation buckle folds developed by the buckling of ice slabs above décollement planes parallel to and up to 3.5 m below the glacier surface (Fig. 7b). Although the major axes of these folds were aligned normal to the flow direction, individual structures had a blister-like form with a central high point and elevation dropping off in all directions. Surface and flow-parallel widths ranged up to 25 m, and a fairly consistent relationship existed between width and slab thickness (Fig. 9). Both initial width and slab thickness were presumably controlled by the magnitude of the longitudinal compressive stress, which would have tended to increase downglacier and towards the glacier margins as the surge propagated into progressively thinner ice. With continued shortening, the folds became upright and isoclinal, and cracks developed along and parallel to the fold hinge. When this happened the limbs frequently collapsed, leaving a surface rubble of ice slabs. Exfoliation buckle folds formed only in the lower glacier where pre-surge ice thicknesses were less than about 70 m (i.e. below 17 km), and they were preferentially developed on topographic flats upglacier from bulge folds. Formation of exfoliation buckle folds seems to have required compressive strain rates in excess of -0.1 day^{-1} (see below).

Thrust faults

Arcuate thrust faults striking normal to the direction of ice flow formed in thin ($\leqslant$30 m) ice reactivated by the surge in June and July 1983 (Fig. 8a). In ice-marginal sections these thrusts were observed to root at the glacier bed (which thus represents a sole thrust) and to cut up-section through the oversteepened downglacier limbs of asymmetric flow folds formed in bed-parallel foliation (Fig. 8b) (this foliation is believed to form during quiescent phase glacier flow by the rotation and shearing of inhomogeneities in the ice—cf. Hudleston & Hooke 1980). Thrusts characteristically dipped upglacier at angles in the region of 40°. Some thrusts could be traced along strike into thicker ice where they merged into bulge folds, which may have overlain blind thrusts at depth (cf. Berger & Johnson 1982, Croot 1987). This implies that the initiation of discrete thrust faults was preceded by a phase of ductile deformation in which asymmetric flow folds were developed in pre-existing foliation (cf. Elliott 1976, Fischer & Coward 1982). This phase of folding may have generated layer orientations favourable for layer-parallel shear, thereby assisting the initiation of thrusting along pre-existing structural weaknesses in the ice. The strike of many thrust faults was parallel to the strike of the local ice foliation.

Thrust faults developed in piggyback fashion (Butler 1982), propagating towards the glacier snout, as a leading imbricate fan to the basal sliding surface. Two types of thrust fault were observed: (i) structures along which total displacements were only a few metres, which were associated with overhanging hangingwalls at the surface (Fig. 8b), and (ii) structures with hangingwall anticlines which were linked along strike to bulge folds, and along which much larger (but unmeasured) displacements occurred (Fig. 7a). Measured displacement rates along active thrust surfaces reached 0.1 m h^{-1} (Fig. 10), and up to 50% of the local shortening around active thrusts was accommodated by motion along the thrust surface. The orientation of slickensides on the emerging thrust surface often indicated that there was a component of oblique-slip motion along the fault, suggesting that its orientation was influenced to some extent by the presence of pre-existing foliation in the ice.

Fig. 7. Surface fold structures developed as the surge front propagated into the terminal lobe of Variegated Glacier in June 1983. (a) A 20 m high bulge fold developed as a hangingwall anticline above the tip of a thrust fault; (b) exfoliation buckle fold.

Fig. 8. (a) Thrust fault cropping out at the glacier surface with overhanging hangingwall. The large boulder on the ice surface initially lay across the fault, and was rolled over by the emergence of the hanging wall. (b) Thrust fault cutting through overturned limb of asymmetric fold in subsurface ice. Section is about 20 m high.


7(b)


8(b)


7(a)


8(a)

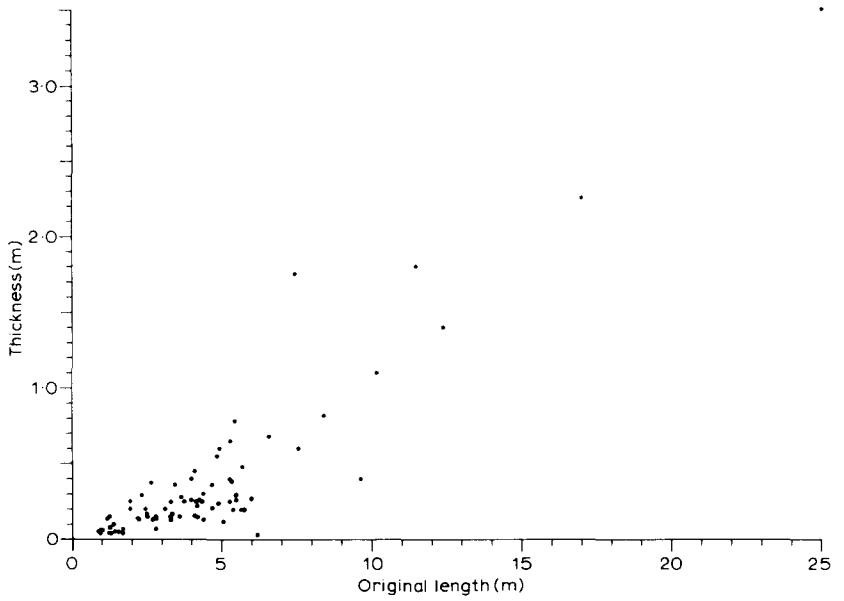

Fig. 9. Plot of the thickness of ice slabs in exfoliation buckle folds against the original length of the ice slab before folding.

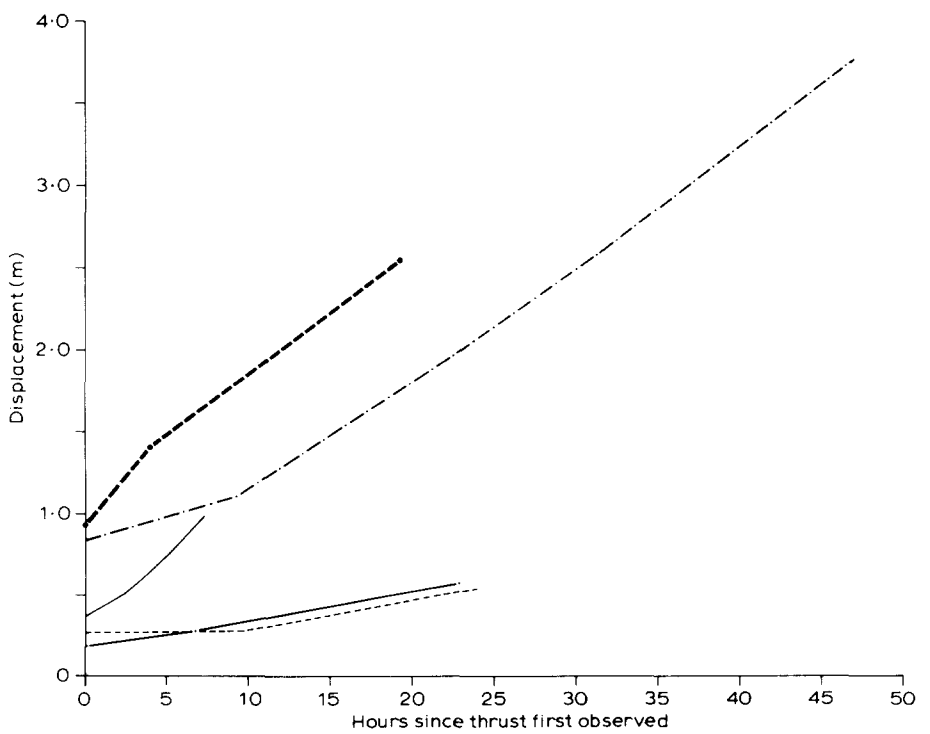

Fig. 10. Plot of the displacements measured along five different active thrust faults emerging at the surface of Variegated Glacier in June 1983.

THE SPATIAL DISTRIBUTION OF ICE STRUCTURES

From the above discussion it is possible to identify three distinct structural zones within the part of the glacier affected by the 1982–1983 surge (Fig. 11). Zone 3 includes that part of the glacier up to 4.5 km from the head, and is a zone of extension tectonics (transverse fractures, marginal wrench faults and net surface lowering). It is associated with areas of the glacier above the surge nucleus which experienced continuous elongation during the surge. Zone 2 lies between 4.5 and 15.5 km from the head of the glacier and is a zone of superimposed compression and extension tectonics (intersecting longitudinal and transverse fractures, marginal wrench faults; net surface lowering in the upper part, net thickening in the lower part). This zone represents that part of the glacier below the surge nucleus through which the surge front and associated velocity peak propagated. It therefore suffered an initial phase of longitudinal shortening, followed by a phase of elongation. Zone 1 is the area below 15.5 km which was always in front of the surge velocity peak. It is a zone of compression tectonics (longitudinal fractures and chasms in the upper part; bulge and exfoliation buckle folds, thrust faults and longitudinal fractures in the lower part; net thickening throughout). Once involved in the surge, this area suffered continuous and large cumulative shortening.

The spatial distribution of structures in Variegated Glacier is therefore explicable in terms of deformation by a strain wave associated with a velocity peak which develops in a limited nucleus zone and propagates through the glacier at a rate faster than the ice itself moves. Compressive tectonic structures develop in front of the velocity peak and extensional structures behind it. Over much of the glacier, downglacier propagation of the velocity peak results in the superimposition of extensional structures onto earlier compressive structures. The nature of the compressive tectonic structures becomes more complex in the lower glacier where the ice being reactivated is relatively thin and the peak strain rates attained are an order of magnitude higher than in the upper glacier.

DEVELOPMENT OF COMPRESSIVE TECTONIC STRUCTURES IN RELATION TO LOCAL PATTERNS OF ICE DEFORMATION

Having established the large-scale relationships between the distribution of structures and the surge-induced deformation history of Variegated Glacier, we now consider the relationships between structures and deformation at a scale of a few metres. In particular we wish to determine:

(a) the relationship between the timing of formation of compressive tectonic structures and the temporal pattern of principal near-surface strain rates;

(b) the relationship between the orientation of compressive tectonic structures and the orientation of the principal axes of near-surface strain; and

(c) the relationship between the location in which specific structures develop and local strain histories.

To do this we established two arrays of markers on the surface of the glacier prior to the arrival of the surge. The location of these arrays (strain nets 1 and 2) is shown in Fig. 6, and their geometry is shown in Fig. 12. Distances between markers in the arrays were measured twice daily with a cloth tape over 4 and 5 day periods during passage of the surge front. Principal near-surface strain rates and strains were calculated from the changes in length of triangle sides using the method of Ramsay (1967, pp. 80–81) as discussed in Raymond *et al.* (1987).

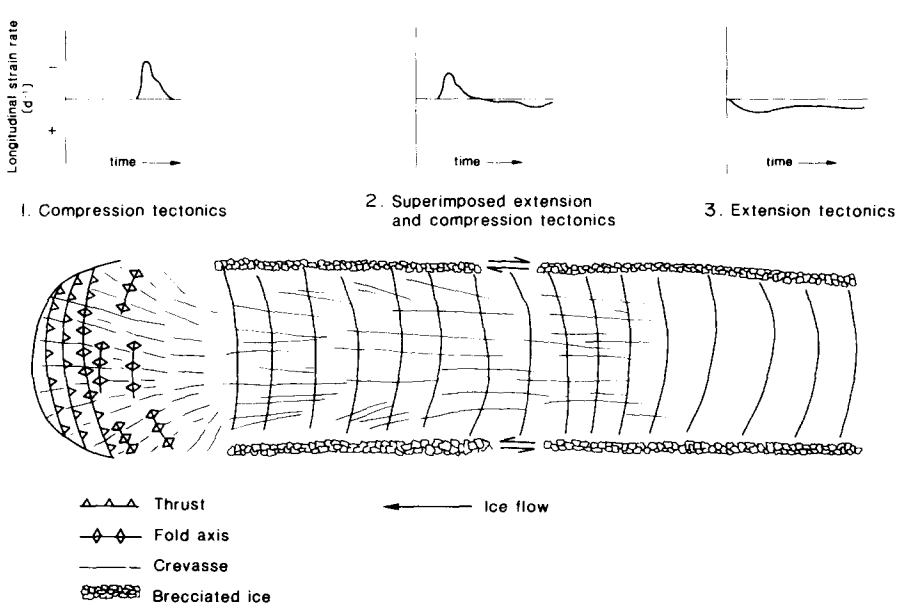

Fig. 11. Schematic diagram showing the distribution of ice structures in a surge-type glacier in relation to the surge-induced deformation histories of the ice.

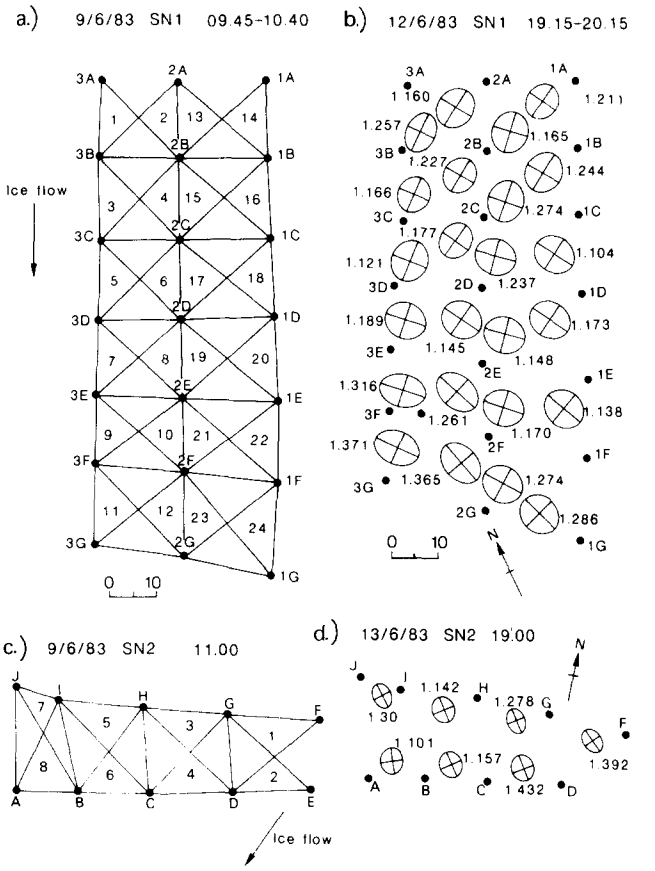

Fig. 12. Geometry of strain nets 1 and 2 at the beginning and end of the periods of measurement. Strain ellipses for individual triangles are also shown, and axial ratios of the ellipses are recorded beside them. Strain within individual triangles is likely to be heterogeneous, so ellipses describe the bulk strain experienced by ice within the triangle. (a) & (b) Strain net 1, (c) & (d) strain net 2. Dates and times of measurements are shown on the diagram.

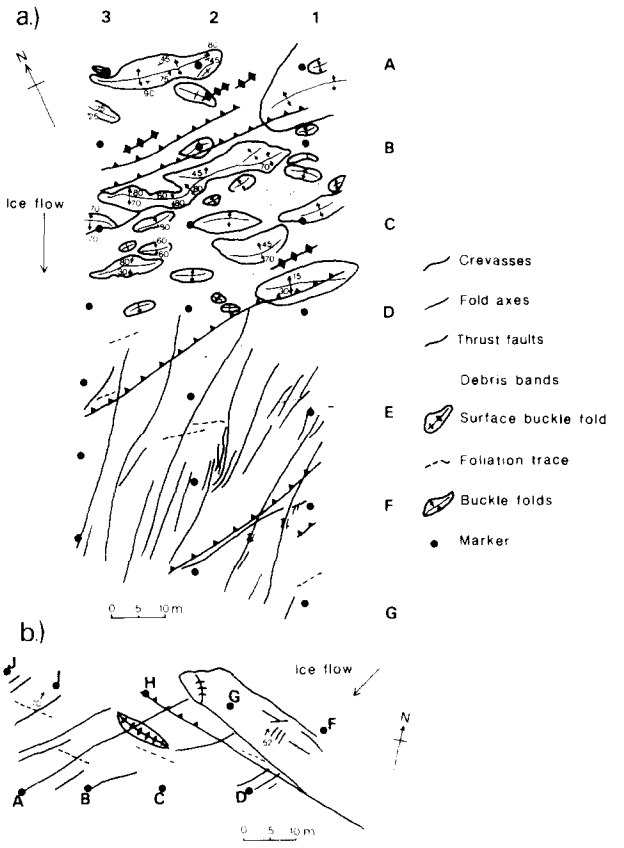

Fig. 13. Maps showing the structures developed in (a) strain net 1, and (b) strain net 2 at the end of the periods of measurement. Apart from foliation and debris bands, all structures mapped developed during the study period. Arrows denote direction and angle of dip of ice surface.

Our convention for principal strain rates is that $\dot{\varepsilon}_1 \geq \dot{\varepsilon}_2$, that extension is positive and that $\dot{\varepsilon}_3$ is always vertical. The method is believed to be able to resolve strain rates in excess of $\pm 0.01\ \text{day}^{-1}$. The timing of development of structures in each net was determined by daily photography of the net, and the distribution and orientation of structures in each net was determined by mapping at the end of each experiment (Fig. 13). Experiments were terminated when the degree of crevassing of the ice surface became so great that sites were no longer accessible.

It is clear from the experiments that the sequence of structure development was bulge folds, thrust faults, exfoliation buckle folds and longitudinal cracks, the latter forming about 1 day after the thrust faults (Fig. 14). Bulge folds continued to develop whilst the other structures were being initiated. Thrust faults formed as principal horizontal compressive strain rates ($\dot{\varepsilon}_2$) reached values of the order of $-0.05\ \text{day}^{-1}$. The other principal horizontal strain rate ($\dot{\varepsilon}_1$) appears also to have been compressive when thrusts were formed (Fig. 14), implying that $\dot{\varepsilon}_3$, the principal vertical strain rate, must have been extensional. Longitudinal cracks formed after $\dot{\varepsilon}_2$ peaked, and as $\dot{\varepsilon}_1$ reached its most tensile value.

Thrust faults formed approximately normal to $\dot{\varepsilon}_2$ and longitudinal cracks normal to $\dot{\varepsilon}_1$, but the two sets of structures were rarely mutually perpendicular (Fig. 13). This was either (a) because the difference in timing of formation of the structures allowed for reorientation of the strain rate axes in the intervening period, (b) because there was a spatial zonation to the development of the two types of structure with strain rate axes being aligned differently in areas occupied by different structures (Figs. 12 and 13), or (c) because the orientation of the thrust faults was influenced by that of pre-existing foliation.

It is clear from Fig. 13 that there was indeed a spatial pattern to the development of structures. This zonation arises because thrust faults and buckle folds tended to develop on topographic flats, whereas longitudinal cracks were associated with topographic ramps. In addition to differences in the orientation of strain rate axes between the two areas, there were differences in strain history (Figs. 15 and 16). In both strain nets thrust faults tended to develop in areas of large shortening ($\varepsilon_2 \simeq -0.1 - -0.2 \gg \varepsilon_1$), which also tended to be areas in which peak compressive strain rates reached $-0.2\ \text{day}^{-1}$. Longitudinal cracks, on the other hand, developed either in areas of low strain or large transverse elongation (Figs. 13 and 16). Peak compressive strain rates in these areas were usually less than $-0.1\ \text{day}^{-1}$ and generally lower than or equal to peak tensile strain rates (Fig. 15).

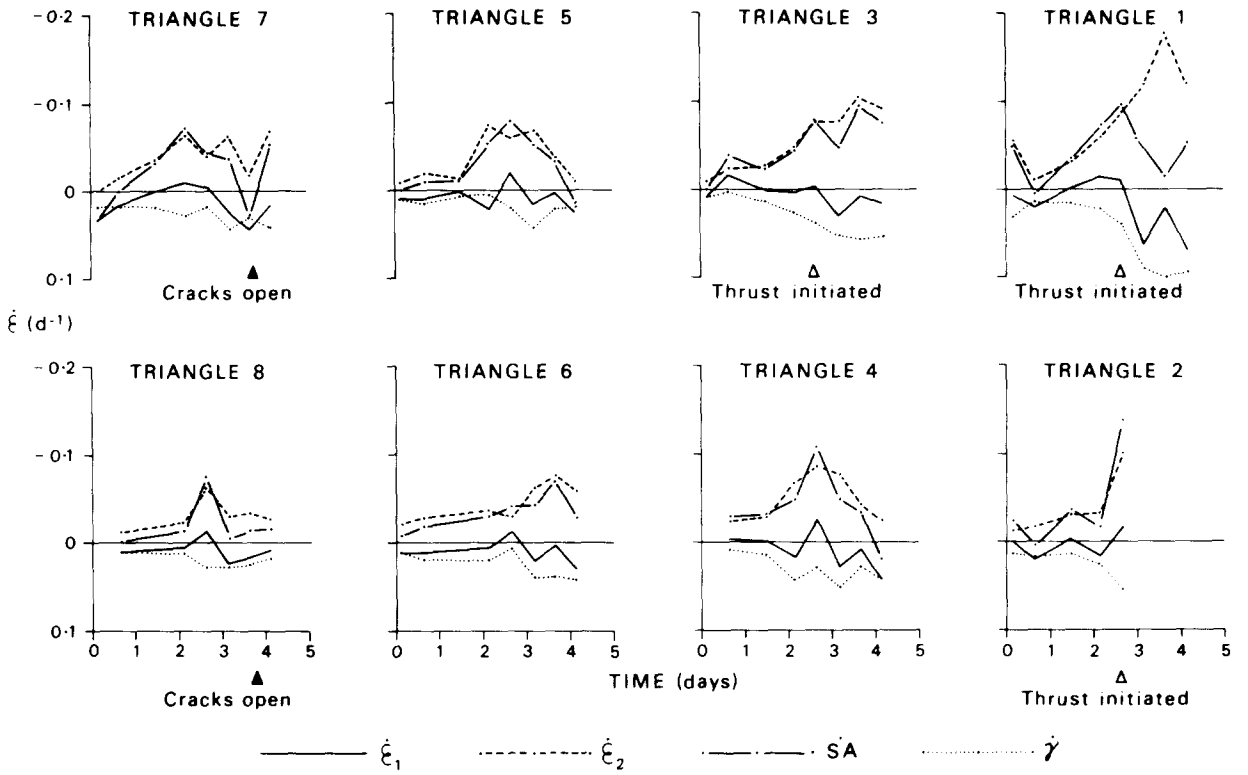

Fig. 14. Temporal pattern of principal near-surface strain rates ($\dot{\varepsilon}_1$ and $\dot{\varepsilon}_2$), areal strain rate ($SA = \dot{\varepsilon}_1 + \dot{\varepsilon}_2$) and shear strain rate ($\dot{\gamma} = (\dot{\varepsilon}_1 - \dot{\varepsilon}_2)/2$) for triangles in strain net 2. Timing of formation of thrust faults and longitudinal cracks is also indicated relative to the pattern of strain in the triangles in which they formed.

Thus, whilst the large-scale distribution of structures was related to the strain produced by movement of the surge front and velocity peak through the glacier, it is clear that local strain histories varied considerably about the large-scale average behaviour. Strain was not homogeneous, even on a small scale, and its heterogeneity is important to the understanding of the details of distribution and orientation of particular types of structure. In particular, the development of structures such as thrust faults, buckle folds and cracks may have been strongly influenced by variations in strain history induced by the growth of larger-scale structural features such as bulge folds. More detailed work would be required to establish these relationships more firmly.

APPLICATION TO GEOLOGICAL SETTINGS

In the above discussion, we have shown how the development, growth and downglacier propagation of the surge velocity peak produced distinctive patterns of ice deformation which are reflected in the character of the ice structures that developed during the surge. In this section we discuss ways in which these observations might shed light on the mechanisms of thrust sheet emplacement and on the relationships between the morphology of a thrust sheet and its deformation history.

It is clear that not one of the three possible mechanisms of thrust sheet emplacement described in the introduction is sufficient to account for the behaviour of Variegated Glacier during its surge. Instead, the dynamics of the surge seem to be best accounted for by a combination of the gravity tectonics and 'push from behind' mechanisms of thrust sheet emplacement. Over much of the length of the surging part of the glacier flow was driven by gravity, but within this region the downslope component of the weight was not fully supported by the local basal shear stress (McMeeking & Johnson 1986). As a result, some of the weight was supported by longitudinal stresses, which were compressive below and extensional above the surge zone. These stresses were transmitted to the glacier bed as a shear stress in the vicinity of discontinuities in basal sliding velocity at the limits of the surge zone (Raymond *et al.* 1987). The resultant stress concentrations enhanced the deformation of ice around the edges of the surge zone, thereby facilitating its propagation. Above the surge zone the ice responded to the stress concentration by fracturing and thinning, thus preventing the occurrence of tectonic denudation. Where the surge propagated into relatively thick ice, this ice responded to longitudinal shortening by thickening and generating the steep slope of the surge front. Where it propagated into thin ice, much larger stress concentrations were produced, sufficient to induce brittle failure of the ice in compression. The surge front then propagated by footwall imbrication as a succession of thrusts developed in piggyback fashion downglacier. In this process, ramping was preceded by a phase of ductile deformation in which asymmetric folds were developed, as suggested by Fischer & Coward (1982). In effect, the surging part of the glacier generated the 'push from behind' which allowed the surge to propagate.

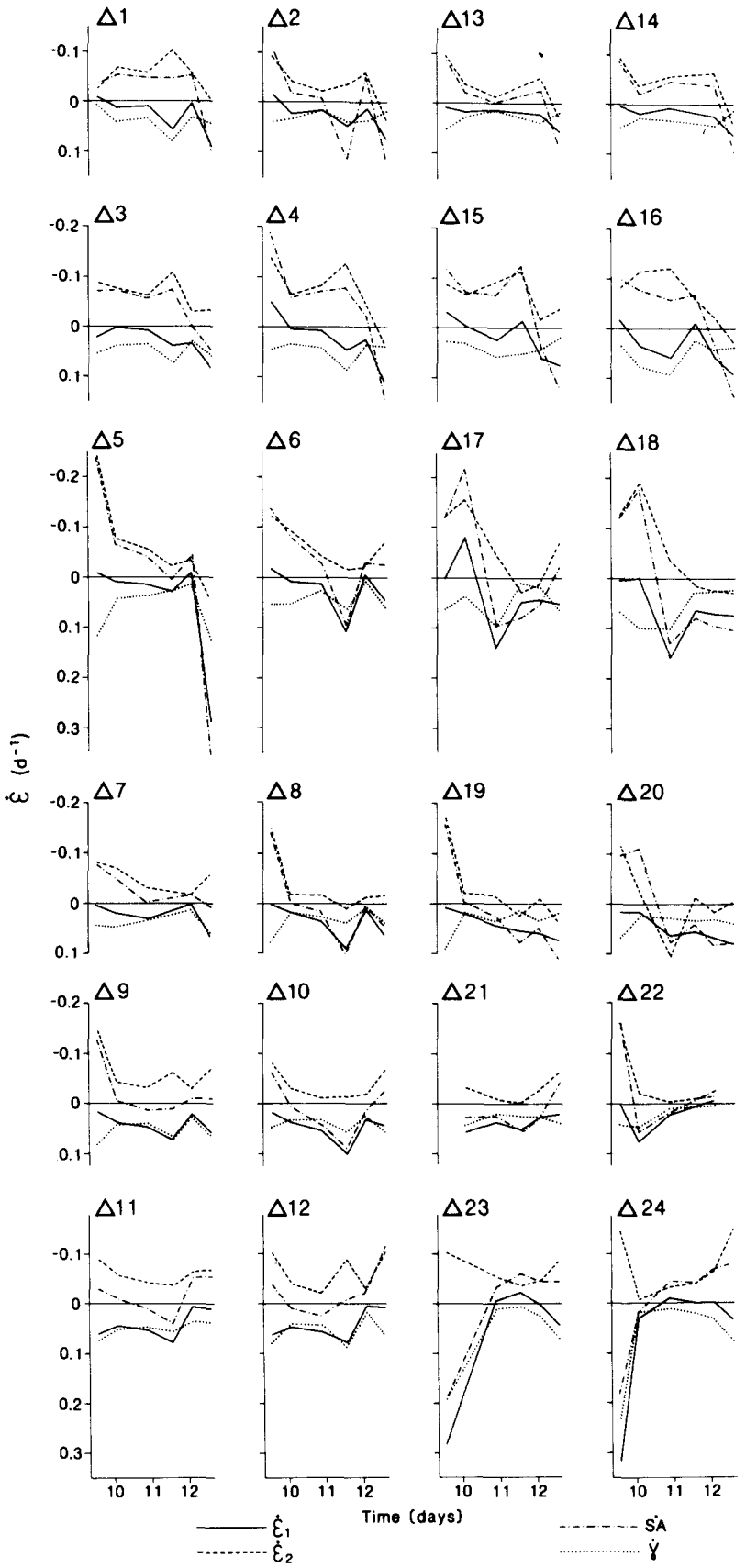

Fig. 15. Temporal pattern of principal strain rates, areal strain rate and shear strain rate for triangles in strain net 1.

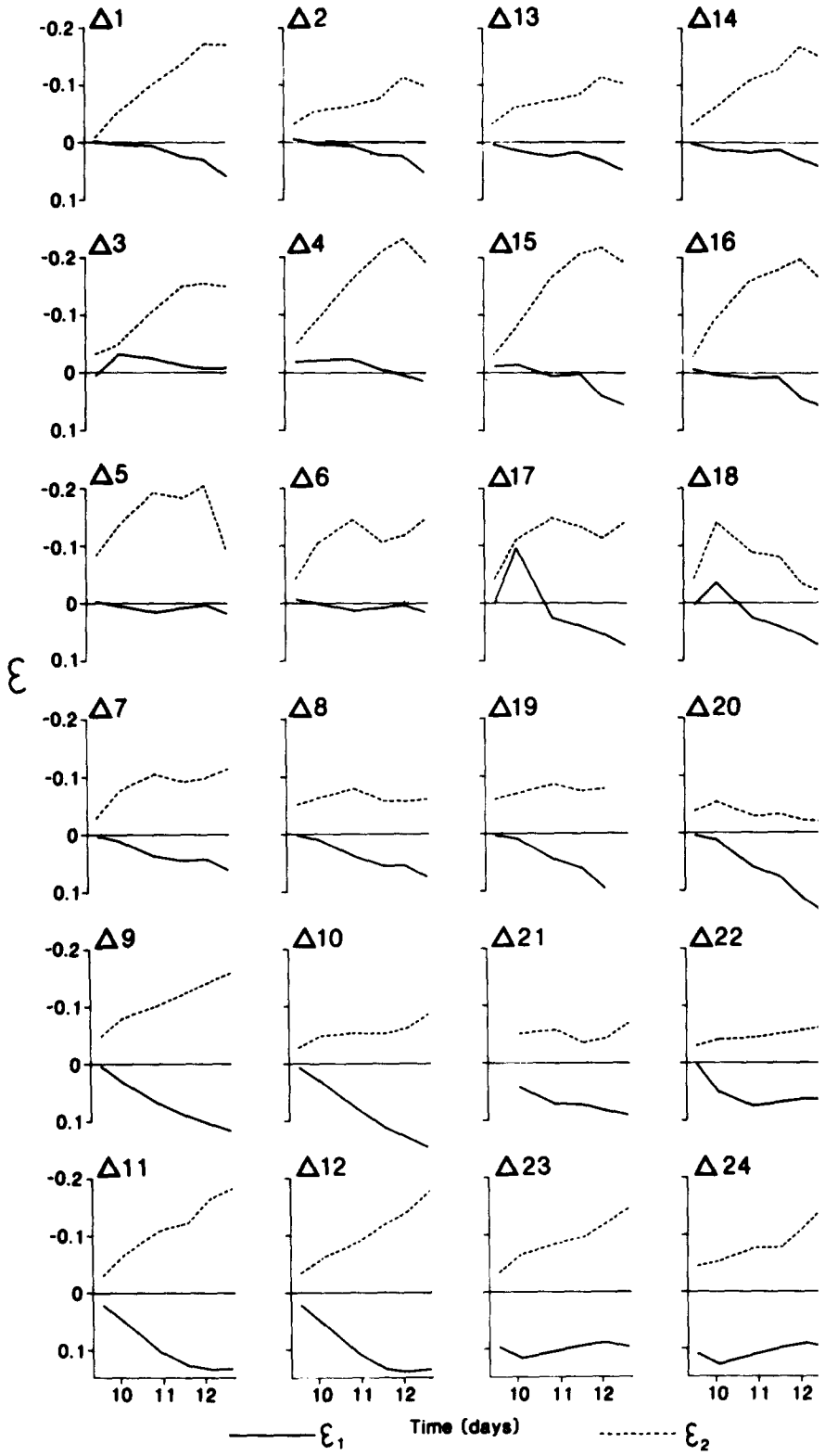

Fig. 16. Principal strains for triangles in strain net 1.

In a surging glacier, it is therefore clear that compressive stresses are not transmitted over the full length of the glacier, but that they are developed only in a limited zone in front of the velocity peak. Their primary effect is to facilitate propagation of the surge front, thereby extending the part of the glacier moving under the influence of gravity. Such a mechanism might well provide an appropriate explanation for the emplacement of thin-skinned fold and thrust belts in rocks. It does not require the overthrust mass to behave as a rigid block, but allows it to attain stability by deforming and creating a 'tectonic wedge' (the surge front) (cf. Chapple 1978).

Many theories of overthrust faulting have tried to overcome the problem of moving the thrust sheet against the resistance of Coulomb friction by postulating motion over a weak basal layer (Hubbert & Rubey 1959, Gretener 1981). This may be a layer of incompetent rock (such as evaporite), some pre-existing structural weakness in the rock body or a layer weakened by high pore fluid pressures, cataclasis or local high temperatures. In the case of Variegated Glacier, direct measurement shows that high water pressures existed beneath the glacier (Kamb *et al.* 1985). These could have facilitated rapid sliding, either by forcing extensive separation between the glacier sole and the subglacial bedrock (Kamb *et al.* 1985), or by weakening and allowing deformation of a layer of permeable subglacial sediments (Clarke *et al.* 1984). In either case, the existence of a weak basal layer would allow the greater part of the surge-induced displacement of most parts of the glacier to occur by gravity-gliding. Flow by plastic deformation was primarily associated with the zones of high longitudinal stress at the upglacier and downglacier limits of the surge zone. Deformation was therefore a transient phenomenon linked to the propagation of strain waves away from the surge nucleus. The idea that many structures develop in relation to the movement of waves of strain through the ice mass may have important implications for the interpretation of structures in rocks.

The structural assemblage described from Variegated Glacier defines a sliding mass with cumulative elongation at its trailing edge, cumulative shortening at its leading edge, and shear along its lateral margins. Within the bulk of the glacier bounded by these marginal areas, structures reflect the superimposed effects of shortening and elongation linked to the downglacier propagation of the surge front. This pattern of cumulative strain and the associated assemblage of structures are very similar to those described from 'surge-zones' of the Moine Thrust zone by Coward (1982). The observations presented here suggest a mechanism of emplacement for such 'surge zones' which involves a combination of gravity gliding and 'push from behind' associated with the propagation of a wave of compressive strain through the rock mass consequent upon the development of a localized sliding instability along the surface which eventually develops into the sole thrust. This mechanism of emplacement also accommodates the model of ramp development proposed by Fischer & Coward (1982), and could be replicated in the formation of the sequences of glaciotectonic structures developed in sediments overridden by surging glaciers, as described by Croot (1987).

Acknowledgements—This work was supported by The Royal Society, The Nuffield Foundation, Merton College, Oxford, and NSF Grants EAR–79–19530 and DPP–82–00725 to the University of Washington. Wendy Lawson acknowledges receipt of a NERC Research Studentship. We are indebted to Professor C. F. Raymond for the opportunity to work at Variegated Glacier and for making available unpublished data concerning the 1982–1983 surge. Fieldwork was carried out with permission of the U.S. National Forest Service (Tongass National Forest) and Park Service (Wrangell-St Elias National Park). Gulf Air Taxi and Livingston Helicopters, Yakutat, Alaska, provided logistic support. Drs M. J. Hambrey, P. J. Hudleston, C. J. Talbot and N. H. Woodcock, and an anonymous reviewer made helpful comments on an earlier draft.

REFERENCES

Berger, P. & Johnson, A. M. 1982. Folding of passive layers and forms of minor structures near terminations of blind thrust faults—application to the central Appalachian blind thrust. *J. Struct. Geol.* **4**, 343–353.

Bindschadler, R., Harrison, W. D., Raymond, C. F. & Crosson, R. 1977. Geometry and dynamics of a surge-type glacier. *J. Glaciol.* **18**, 181–194.

Butler, R. W. H. 1982. The terminology of structures in thrust belts. *J. Struct. Geol.* **4**, 239–245.

Chapple, W. M. 1978. Mechanics of thin-skinned fold-and-thrust belts. *Bull. geol. Soc. Am.* **89**, 1189–1198.

Clarke, G. K. C., Collins, S. G. & Thompson, D. E. 1984. Flow, thermal structure and subglacial conditions of a surge-type glacier. *Can. J. Earth Sci.* **21**, 232–240.

Collins, I. F. & McCrae, I. R. 1985. Creep buckling of ice shelves and the formation of pressure rollers. *J. Glaciol.* **31**, 242–252.

Coward, M. P. 1982. Surge zones in the Moine thrust zone of north west Scotland. *J. Struct. Geol.* **4**, 247–256.

Croot, D. G. 1987. Glacio-tectonic structures: a mesoscale model of thin-skinned thrust sheets? *J. Struct. Geol.* **9**, 797–808.

Elliott, D. 1976. The motion of thrust sheets. *J. geophys. Res.* **81**, 949–963.

Fischer, M. W. & Coward, M. P. 1982. Strains and folds within thrust sheets: an analysis of the Heilam sheet, Northwest Scotland. *Tectonophysics* **88**, 291–312.

Gretener, P. 1981. Pore pressure, discontinuities, isostasy and overthrusts. In: *Thrust and Nappe Tectonics* (edited by McClay, K. R. & Price, N. J.). *Spec. Publs geol Soc. Lond.* **9**, 33–39.

Hambrey, M. J. & Milnes, A. G. 1977. Structural geology of an Alpine glacier. *Eclog. geol. Helv.* **70**, 667–684.

Hubbert, M. K. & Rubey, W. W. 1959. Role of fluid pressure in the mechanics of overthrust faulting. *Bull. geol. Soc. Am.* **70**, 115–166.

Hudleston, P. J. 1977. Similar folds, recumbent folds and gravity tectonics in ice and rocks. *J. Geol.* **85**, 113–122.

Hudleston, P. J. & Hooke, R. Le B. 1980. Cumulative deformation in the Barnes Ice Cap and implications for the development of foliation. *Tectonophysics* **66**, 127–146.

Kamb, W. B., Raymond, C. F., Harrison, W. D., Engelhardt, H. F., Echelmeyer, K. A., Humphrey, N., Brugman, M. M. & Pfeffer, T. 1985. Glacier surge mechanism: 1982–1983 surge of Variegated Glacier, Alaska. *Science* **227**, 469–479.

McMeeking, R. M. & Johnson, R. E. 1986. On the mechanics of surging glaciers. *J. Glaciol.* **32**, 120–132.

Meier, M. F. & Post, A. S. 1969. What are glacier surges? *Can. J. Earth Sci.* **6**, 807–819.

Price, N. J. & McClay, K. R. 1981. Introduction. In: *Thrust and Nappe Tectonics* (edited by McClay, K. R. & Price, N. J.). *Spec. Publs geol. Soc. Lond.* **9**, 1–5.

Ramsay, J. G. 1967. *Folding and Fracturing of Rocks*. McGraw-Hill, New York.

Raymond, C. F. 1987. How do glaciers surge? A review. *J. geophys. Res.* **92**, B9, 9121–9134.

Raymond, C. F. & Harrison, W. D. In press. Progressive changes in geometry and velocity of Variegated Glacier prior to its surge. *J. Glaciol.*

Raymond, C. F., Johannesson, T., Pfeffer, T. & Sharp, M. 1987. Propagation of a glacier surge into stagnant ice. *J. geophys. Res.* **92**, B9, 9037–9049.